IMPLEMENTATION OF THE ANN MODEL TO A COMPLICATED DRAINAGE SYSTEM

NOBUAKI KIMURA
Institute for rural engineering, National Agriculture & food Research Organization, Tsukuba, Japan, kimuran590@affrc.go.jp

IKUO YOSHINAGA
Institute for rural engineering, National Agriculture & food Research Organization, Tsukuba, Japan, yoshi190@affrc.go.jp

KENJI SEKIJIMA
Institute for rural engineering, National Agriculture & food Research Organization, Tsukuba, Japan, sekijimak436@affrc.go.jp

ISSAKU AZECHI
Institute for rural engineering, National Agriculture & food Research Organization, Tsukuba, Japan, issaku@affrc.go.jp

DAICHI BABA
ARK Information Systems, INC., Tokyo, Japan, baba.daichi@ark-info-sys.co.jp

ABSTRACT

Automatic and adaptive pumping operations on drainage management in a lowland have been required to reduce run costs on efficient, regular pumping and promote effective water-supply for paddy fields and proper controls for flood events. To satisfy these requirements in controlling the entire water volume in the lowland, an effective and efficient, real-time prediction model is required. The model is usually run using observed data from the fields. For a sustainable operation with reduction of run cost and manpower, this study focused on investigating minimum observed instruments based on locations and data items to maintain accurate model predictions. We employed the long short-term memory (LSTM) model as a data-driven model, which can predict long-term, time-series data accurately. The LSTM model that predicts water level and discharge was implemented to a mid-size agricultural lowland with a complicated drainage system. In the area, several stations for intake (four irrigation pumping stations) and for drainage (five drainage pumping stations), numerous canals and a regulating pond exist. Continuous, long-term observed data are available. Water level predictions were conducted with a variety of cases with different inputs based on the number of stations and the combinations of data items (e.g., water level & rainfall, and water level & drain discharge) during April to August (irrigation season). The error evaluation was conducted by K-fold cross-validation. The results showed that the information of water level as input data was greatly crucial for accurate outputs and that four irrigation pumping stations and a main drainage pumping station were proper to minimize observed locations during irrigation season.

Keywords: ANN model, long short-term memory, drainage system, water level

1. INTRODUCTION

Drainage pumping has an important role to control water volume in a lowland to dry out wetlands. When pumps are run or stopped based on some regional rules of drainage management, some drainage pumping stations still employ human-judgment operation, some automatically operate the pumps using real-time systems that monitor water level in a regulating pond near a pumping station, and the others perform mixed operation based on human-based and automated judgments. It is necessary to introduce an effective and efficient, real-time monitoring and forecasting system to support various pumping operations. In general, monitoring systems require observational instruments coupled with information communication technology tools, key locations for monitoring, and crucial variables of data items. These systems are extremely expensive to maintain continuous operations. If minimum locations (e.g., pumping stations and canals) and minimum variables of data items (e.g., water level, rainfall, and pump discharge) for monitoring are determined, pumping operations by managers and even automatic systems would become more effective and efficient. Moreover, the operational and maintenance fees would be reduced. It is necessary to investigate what an effective and efficient monitoring system is.

To provide an appropriate answer for this kind of question, physical-based models such as conceptional hydraulic models and hydrological models usually can be used to simulate the entire water volume of a lowland and water level in a pond. However, those models require hard work such as creation of calculational meshes and determination of geological and hydrological parameters in the preprocessing. Instead, we focus on using a deep neural network (DNN) model to investigate what effective and efficient monitoring systems are required

in an actual lowland. This is because the DNN model is one of the data-driven models and is able to run only using past data without any setups of physical features in the lowland. DNN models have been applied to riverine flood simulations (e.g., Hitokoto et al., 2016). These models are created based on multilayer perceptron (MLP), one of the conventional neural networks originally proposed by McCulloch and Pitts (1943). Different types of DNN models has been recently utilized to predict water level and discharge in riverine flood events. For example, a long short-term memory (LSTM) model originally proposed by Hochreiter and Schmidhuber (1997) were applied to regional flood events using the observed datasets (Yamada et al., 2018; Hu et al., 2018; Le et al., 2019). As the results of these studies, the LSTM model is greatly beneficial to predict time-series data based on the evaluation of prediction accuracy. These studies were conducted in specific rivers over local watersheds.

Our study needs to predict time-series water levels in a pond that has a role of adjusting water volume in a lowland. Kimura et al. (2019) already developed MLP and LSTM models to predict water level and discharge for drainage management in small- to middle-size lowlands. They also revealed that LSTM model predicted more accurate water levels and discharges than those by the MLP model. For example, using the observed data, including several severe flood events, for approximately eight years in a middle-size lowland, the predicted water level by LSTM model was more accurate by 2–6% than that by the MLP model up to three-hour lead time. As our target study site is used primarily for paddy fields, irrigation season (spring to summer) is crucial to control water volume for the fields. Therefore, it is necessary to provide the accurate information of water level in the pond. Although Kimura et al. (submitted manuscript, 2020) have already investigated what kind of input datasets for the LSTM model provide more accurate performance for continues, long-term predictions, they did not conduct the model validation during specific periods such as irrigation season and flood season. However, a target period is the irrigation season in this study focused. In addition, it is necessary to investigate what function of a monitoring system is appropriate through effective and efficient operations of pumps.

The purposes of this study are first to verify a better accuracy of the LSTM model rather than that of the MLP model during the irrigation season, and secondly to perform sensitivity tests of LSTM model for minimizing monitoring points and data items over a lowland, and finally to propose an appropriate monitoring system based on accuracy evaluation of the model.

2. METHOD

2.1 Study site

The target lowland is located in a northern portion of Central Japan, close to a coast line on the north side and enclosed by three rivers on the other sides. The lowland has an area of approximately 100 km^2 and a small pond (approximately 1.5 km^2) in the northwest part that is used to control the entire water volume of the area (Figure 1). The lowland has main five drainage pumping stations and main four irrigation pumping stations (Table 1). The largest drainage pumping station (D2) is directly connected to the pond with a wide canal without slope and always works to maintain water level in the pond. The other drainage pumping stations (D2 –D5) potentially work from April to October during heavy rainfall events. The irrigation pumping stations (I1–I4) work from May to August for rice-paddy cultivation. Each pumping station provides the data, including water level, rainfall, and discharge that the pumps drain or draw.

2.2 Conventional neural network

A MLP model, one of the conventional neural network models, consists of three layers—input layer, hidden layer, and output layer—and makes network with nodes as a brain model. The hidden layer can be extended to several layers. Each node has an activation function that filters input values x with weighted coefficients w into an output value Y. If a layer has n nodes, a certain node k in a subsequent layer receives n input values. These inputs weighted by coefficients are integrated and added by a bias b_k. The activation function $F(*)$ outputs Y_k from a node. These variables are defined in the following equations.

$$y_k = \sum_{j=1}^{n} w_{j,k} x_j + b_k, \tag{1}$$

$$Y_k = F(y_k), \tag{2}$$

The network structure of the MLP model and the inner structure of the node are shown in Figure 2 when two variables (A and B) are used as input data. The variables are predicted at the forward time step $(t + 1)$ in the output layer.

2.3 Long short-term memory (LSTM) model

A LSTM model is a type of RNN architecture and is proper to train the data that have long-term trends. The LSTM model was created to solve problems in vanishing and exploding gradients by introducing a memory cell. For the LSTM inner structure (Fig. 2a), input data x_t at present time t are mixed with output data h_{t-1} at the

previous time step $t-1$. The input data move to three gates: forget, input, and output. A function of the forget gate f_t that removes some information from the memory cell is defined as the following equation.

$$f_t = \sigma\left(w_f[h_{t-1}, x_t] + b_f\right) \tag{3}$$

where $w_f[h_{t-1}, x_t]$ is a matrix operation related to x_t and h_{t-1}; b_f is a bias; and σ is a sigmoid as an activation function. The input gate mixes two types of information sources, obtained from feature quantities of the input data with two different activation functions. The two sources are expressed in Equations (2) and (3). The input gate adds the mixed information to the memory cell.

$$i_t = \sigma(w_i[h_{t-1}, x_t] + b_i), \tag{4}$$

$$z_t = \tanh(w_z[h_{t-1}, x_t] + b_z), \tag{5}$$

where tanh is a hyperbolic tangent as an activation function, and b_i and b_z are biases. The variables f_t, i_t, and z_t are combined into the following equation with the state of a past trend at $t-1$ (C_{t-1}) that a memory cell holds.

$$C_t = f_t \otimes C_{t-1} \oplus i_t \otimes z_t, \tag{6}$$

where $\otimes$ is multiplication; and $\oplus$ is addition. The output gate function o_t that still involves the original feature quantities of the input data is defined in the following equation.

$$o_t = \sigma(w_o[h_{t-1}, x_t] + b_o), \tag{7}$$

where b_o is a bias. Finally, the C_t from the memory cell is multiplied by o_t and updates the output (h_t)

$$h_t = o_t \otimes \tanh(C_t). \tag{8}$$

A network structure of the LSTM model has three layers: input, hidden, and output. The hidden layer can be extended to several layers. Figure 3 shows the network and inner structures of the LSTM model.

2.4 Simulation designs

This study focused on the temporal prediction of water level at a pond connected to the main drainage pumping station (D1) through a wide canal. The water level at D1 was set up as a model output because there is no slope between the pond and D1 in water level. The data at drainage- and irrigation-pumping stations were used for the sensitivity tests as model input. Each station collected the data that consist of major three variables: rainfall, water level, and pump discharge (hereafter "discharge"). The run of the LSTM model with the input data at all stations and three variables at each station was defined as a basic case (Case 1). For a model comparison between LSTM and conventional neural network models, the MLP model was run with the same calculation condition in Case 1. This is defined as Case 0. The role of the irrigation pumping stations (I1–I4) for predicted water level in D1 should be clarified because a prediction period is the irrigation season. Cases 2–9 were performed without the drainage pumping stations except for D1. Case 2 has I1–I4 and D1 to clarify the effect of the irrigation pumping stations on the predicted water level. This is because D2–D5 are used primarily for heavy rainfall events. In reality, only a few heavy rainfall events usually occur for a year. Cases 3–5 tested a combination of two variables like "water level and rainfall" or "water level and discharge" as input data. Cases 6–8 were tested to select only one variable. Case 9 used only D1's water level as input to test the effect of the water level of D1 on the prediction. Case 10 was tested only using water levels of the irrigation pumping stations. One run by the MLP model was conducted and the LSTM model ran the nice cases listed in Table 2.

2.5 Data acquisition, model validation, and data flow

The observed data at all pumping stations were obtained at the target lowland from 2010 to 2017. The data were selected only from April to August for the irrigation season in paddy fields. Some data from a drainage pumping station were collected and preserved by the Ministry of Land, Infrastructure, Transport, and Tourism in Japan (MLIT Japan). The other data were obtained by a local social association for land development, in cooperation with a local government and the Ministry of Agriculture, Forestry and Fisheries of Japan (MAFF Japan). Missing data were interpolated. These data were used to train the LSTM model and to evaluate the errors of model predictions. K-fold cross-validation (Geisser, 1993) was utilized for the validation comparison. The number K was set to eight, and the observed data were separated into eight groups. Seven groups were used for training the model and one group was used for comparison with the model prediction. The one group for model prediction was exchanged with the other groups in order. A quantitative error between observation and prediction was defined by root mean square error (RMSE). A mean RMSE (M-RMSE) that is averaged over the RMSEs from eight-time tests, each of whose was conducted in each group, was adopted for a comparison among

all cases listed in Table 2. The second group (G2) of the eight groups was also considered for RMSE evaluation because it involves the highest flood peak during the observed period.

Observed data were obtained from the field measurements in the first step. Parts of the observed data were used for the cross-validation in a learning process in the second step. In the third step, the remainder of the observed data were used for prediction. The data flow for the procedures in learning and prediction by the LSTM model is illustrated in Figure 4. The program for the LSTM model was created using Python (version 3.6.4, www.python.org) incorporated with the Python deep learning libraries in Keras (keras.io/ja) on a Windows-OS PC with an Intel Core i7-4770K CPU at 3.50 GHz. The setups of several hyperparameters, such as batch size and epoch number, and of the functions such as activation function and error evaluation, are detailed in Table 3. These hyperparameters were calibrated in the former study (Kimura et al. submitted manuscript, 2020).

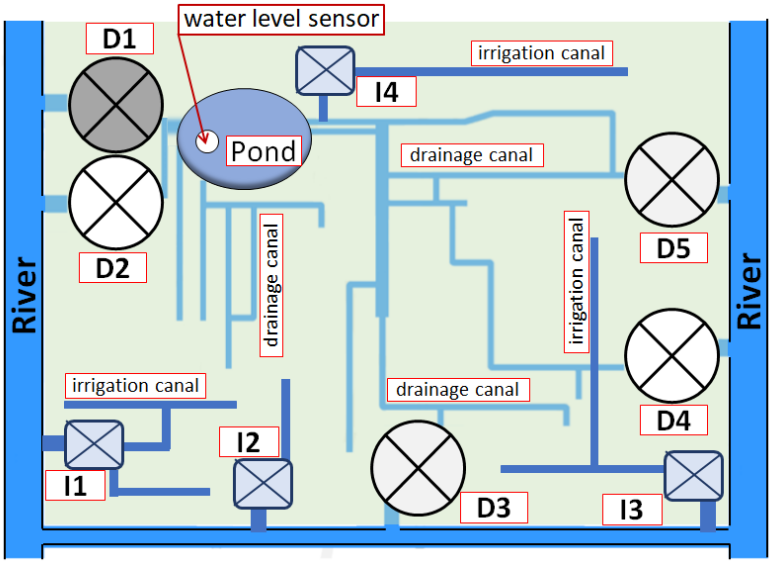

Figure 1. Map of a field site, showing a pond, drainage pumping stations (D1–D5), irrigation pumping stations (I1–I4), and major drainage and irrigation canals.

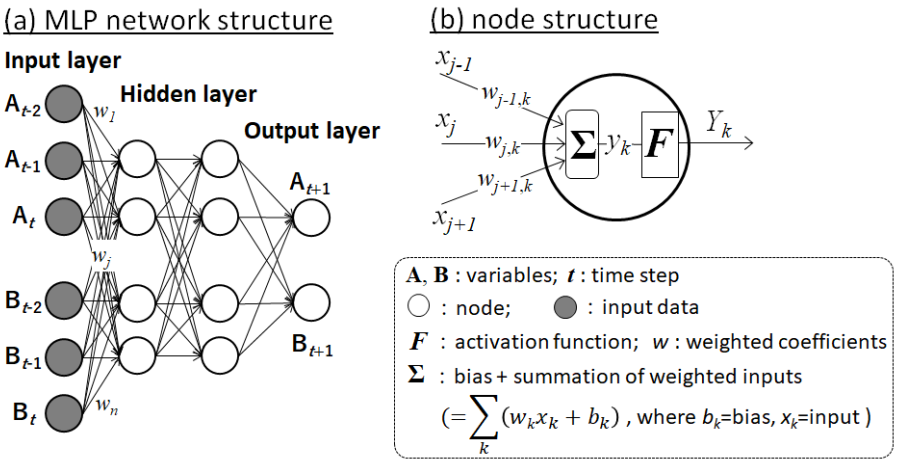

Figure 2. Network and node structures in the MLP model. (a) a network structure is an example of time-series A and B variables with time steps (t-2 to t+1). (b) node k has inputs (j-1 to j+1) with weighted coefficients, sums up them, passes through the activation function, and makes the output.

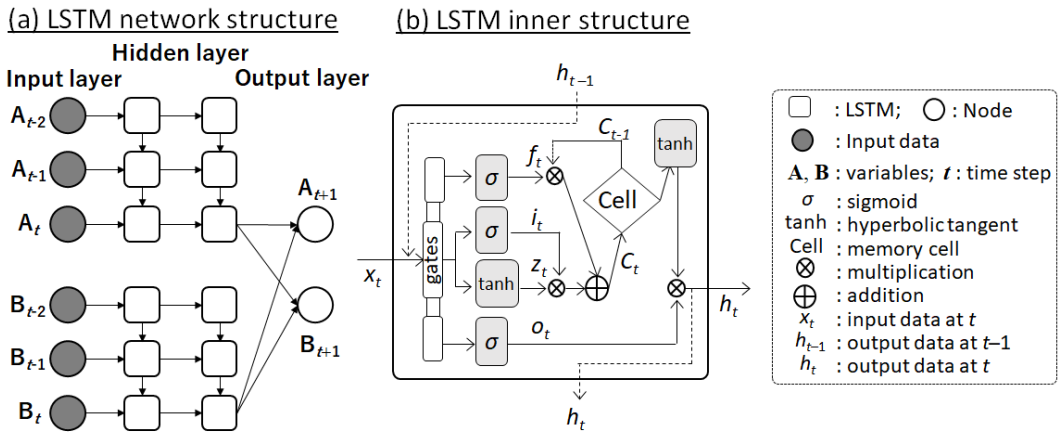

Figure 3. Network and inner structures of a LSTM model. (a) network has two layers in the hidden layer with two variables (A and B) in time-series data. (b) inner structure has three gates with a memory function (Cell) that hold past trends.

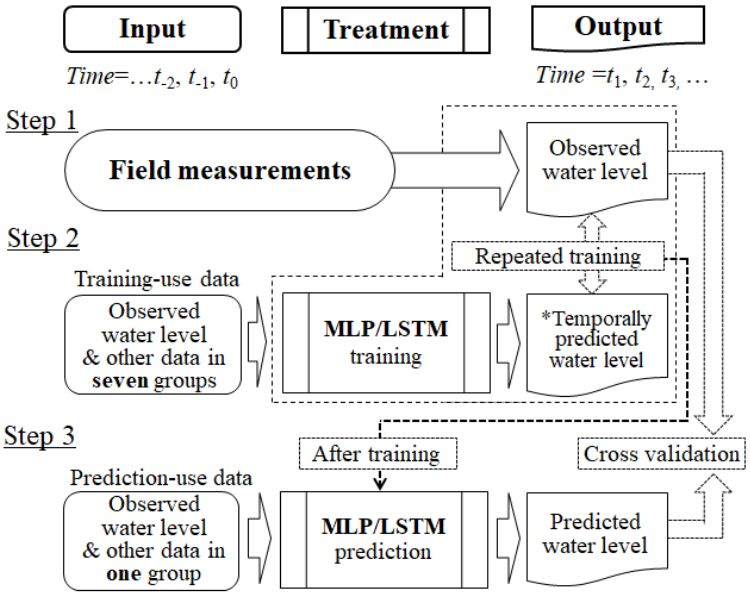

Figure 4. Data flow for training and prediction by MLP and LSTM models.

Table 1. Characteristics of the major pumping stations (I1–I4 for irrigation and D1–D5 for drainage).

	I1	I2	I3	I4	D1	D2	D3	D4	D5
The number of pumps	3	2	2	2	4	2	3	3	3
Maximum flow rate (m^3/s)	5.9	4.2	8.4	2.2	60.0	40.0	6.8	12.8	16.2

Table 2. Simulation cases for sensitivity tests

	Data type	Case 1	Case 2	Case 3	Case 4	Case 5	Case 6	Case 7	Case 8	Case 9	Case10
	Water level	○	○	○	○		○				○
I1	Rainfall	○	○	○		○		○			
	Discharge	○	○		○	○			○		
	Water level	○	○	○	○		○				○
I2	Rainfall	○	○	○		○		○			
	Discharge	○	○		○	○			○		
	Water level	○	○	○	○		○				○
I3	Rainfall	○	○	○		○		○			
	Discharge	○	○		○	○			○		
	Water level	○	○	○	○		○				○
I4	Rainfall	○	○	○		○		○			
	Discharge	○	○		○	○			○		

	Water level	○	○	○	○		○				○	
D1	Rainfall	○	○	○		○		○				
	Discharge	○	○		○	○			○			
	Water level	○										
D2	Rainfall	○										
	Discharge	○										
	Water level	○										
D3	Rainfall	○										
	Discharge	○										
	Water level	○										
D4	Rainfall	○										
	Discharge	○										
	Water level	○										
D5	Rainfall	○										
	Discharge	○										

Table 3. Setups of hyperparameters and functions for MLP and LSTM models

Hyperparameters/functions	Values/function	Remarks
Number of hidden layers	2	
Number of vector dimensions (or nodes) in inner parameters	20	The number of nodes in hidden layer (Figure 2a) or the vector of C_t (Figure 3b)
Past and present time in input	−6 to 0	Time interval = h
Lead time in output	1, 3, 6	Time unit = h
Batch size	100	
Number of epochs	100	
Learning rate	0.01	For SGD implementation
Dropout rate	0.0	
Reproducibility	None	
Optimizer	Stochastic gradient descent (SGD)	
Activation function	Sigmoid or hyperbolic tangent	Used in nodes or inner structures of the LSTM model
Loss function in training processes	Mean square error $= \frac{1}{N1}\sum_{j=1}^{N1}\left(V_{cj} - V_{oj}\right)^2$	c_i=model prediction, o_i= observed data, *N1*=the number of data
Error evaluation in cross validation	Root mean square error (RMSE) $= \sqrt{\frac{1}{N1}\sum_{j=1}^{N1}\left(V_{cj} - V_{oj}\right)^2}$	Same as above
Error evaluation	Relative error (RE) $= \frac{1}{N1}\sum_{j=1}^{N1}\frac{\lvert V_{cj} - V_{oj}\rvert}{Voj}$	Same as above

3. RESULTS & DISCUSSION

Water levels and rainfalls collected in the field from 2010 to 2017 as inputs of the DNNs are shown in Figure 5 during irrigation season (April to August) in each year (i.e., group). Severe flood events (>25 mm/h for rainfall) seldom occurred for these periods. Ten severe rainfall events with over 25 mm/h occurred during the irrigation period of the eight years. In Figure 5b, G2 had the largest flood event (approximately 40 mm/h for the rainfall intensity). Note that for the DNN simulations, missing data such as water level and rainfall were set up to constant values in the group 6 (Figure 5f).

Figure 6 shows predicted water levels in G2 in lead times 1, 3, and 6 h of Cases 0 and 1, compared with the observed data (water levels and rainfalls). The LSTM model performed accurate predictions of water levels in 1 h- and 3 h-lead times even during the flood event as well as a normal event in two small panels. However, the precited water level in 6 h lead time was worse because each peak cannot be captured potentially due to time lag of 6 h. For quantitative evaluation, the predicted water levels in G2 simulated by the LSTM model (Case 1) provided reasonable RMSEs of 0.033–0.067 m in 1–6 h lead times corresponding to 3.0–6.0% of maximum gap of observed water level. These RMSEs were slightly better than those by Case 0 (MLP model) with 8–35% improvements. In addition, the relative errors (REs) in G2 in the lead times were 8.1–15.3%. From the cross validation, M-RMSEs averaged over all groups were 0.027–0.051 m in the lead times. These values were

slightly better than those of G2 because G2 involves the highest peak of water level, which is hard to be accurately predicted due to no similar peaks in a training process among the other groups. The REs for all groups in Case 1 were 5.5–8.2% in the lead times, which indicates that the predictions by the LSTM model were reasonable over the all groups. The previous study (Kimura et al. 2019) reported that the MLP model with one hidden layer provided RE = 10.8% up to 3 h-lead time for 8-year simulation. The model accuracy in this study was slightly better than the of the previous one because of using the LSTM model as an advanced model.

For the model sensitivity tests among the observed locations and the variables of data items, Cases 2–10 were run with the same computational condition of Case 1 except for input data. The RMSEs in lead times from the Case-1 run were utilized as the base values when compared with the other cases. A difference from the Case-1 error was defined as the following equation to evaluate relative comparisons of M-RMSE and G2-RMSE among Cases 2–10 when those of Case1 are one.

$$\text{Difference } = 100 \times (\text{RMSE}_{Other\ case} - \text{RMSE}_{Case1})/\text{RMSE}_{Case1} \quad (9)$$

where RMSE is replaced by M-RMSE or G2-RMSE. Figure 7 indicates the differences among Cases 2–10 and adds the difference of Case 0 as a reference. The differences of Case 2 were slightly reduced by 1.3–3.3% from those of Case 1 in M-RMSE and were improved by 9.3% and 1.3% for 1 h- and 3 h-lead times in G2-RMSE but almost equivalent for 6 h-lead time. The differences in Cases 3 and 4 with water level as input data were slightly worse than those of Case 2. This suggests that three variables at all irrigation pumping stations and the main drainage pumping station are enough to perform accurate predictions. Cases 5, 7, and 8 that did not include water level as input data in I1–I4 and D1 provide larger differences by more than 10% of Case 1 in both error evaluations of RMSEs, indicating that worse predictions of water level were provided. Moreover, Case 10 without the water level at D1 as the input also predicted water level poorly by more than 8%. As a result, water level was a key variable as input. The differences in 6 h-lead time among Cases 5, 7, 8, and 10 were reduced from those of the other lead times. This result indicates that even Case 1 must have simulated poorly in 6 h-lead time. Therefore, the differences between those four cases and Case1 were relatively small in a longer lead time.

The error evaluation with RMSEs might not be proper to measure the accuracy of a model that simulate zigzag shapes of water level produced by repeating on-/off-pumping operation like this study. We assumed that RMSEs for gradients of water level per time step could measure the zigzag shape. The RMSEs were separated with three patterns based on the same, opposite, and neutral (zero) directions across time axis of the gradients between observed and predicted data. That is, if two gradients by observed and predicted water levels are positive together or negative, the gradients have the same direction. On the other hand, the two gradients are negative and positive and vice versa, it is defined as he opposite direction. The neutral direction means that at least one gradient is zero. The ratios to the occurrences for the same, opposite, and neutral directions of the gradients were 1, approximately 1, and approximately 0.5 respectively if the number of the same direction was defined as one. Figure 8 shows the differences in Eq. (9), calculated by RMSEs of gradients in three types of directions. In the same direction of observed and predicted gradients, Cases 2–4 predicted a more similar shape of the observed water level due to the reduction of the differences from Case 1 except for the difference of the 1 h-lead-time in Case 3 (Figure 8a). Cases 5, 8, and 10 were worse and Case 7 was the worst. These outputs support the results of Figure 7. For the opposite direction of gradients in Figure 8b, Cases 5, 7, 8, and 10 were better by more than 15% than Case 1. These results can be explained by the following reason. Because these cases predicted relatively small amplitudes of water level across time axis, the gaps between the observed and predicted gradients in the opposite direction were also relatively small when compared with the gap of Case 1. The neutral direction shows that the gradient gaps in Cases 2–4 were similar to those of Case 1 (Figure 8c). However, Cases 5, 8 and 10 provided smaller gaps of gradients when compared with those of Case 1. These outputs were consistent with the results of Figure 8b. Case 7 provided the worst, which was not consistent with the differences of Case 7 of Figure 8b. This can be explained by the following description. Case 7 used only rainfall as input data that did not often occur in reality. Most data from rainfall were zero and weakly responded to the temporal changes of water level. The impact of the neutral direction on the prediction of zigzag shapes of water-level amplitudes were weaker than the other directions of gradients because the number of the neutral direction was small. Note that the ratios of three directions of gradients are unable to be simply added with the percent of the differences in Figures 8a, b and c because those percent are averaged values over the number of the occurrences in each direction. With the introduction of the RMSEs of gradients between observed and predicted water levels, the shapes of amplitudes could be evaluated. As a result, we revealed that Case 2 performed a more accurate prediction of water level through the error evaluation of amplitude shapes as well as RMSEs between observed and predicted water levels.

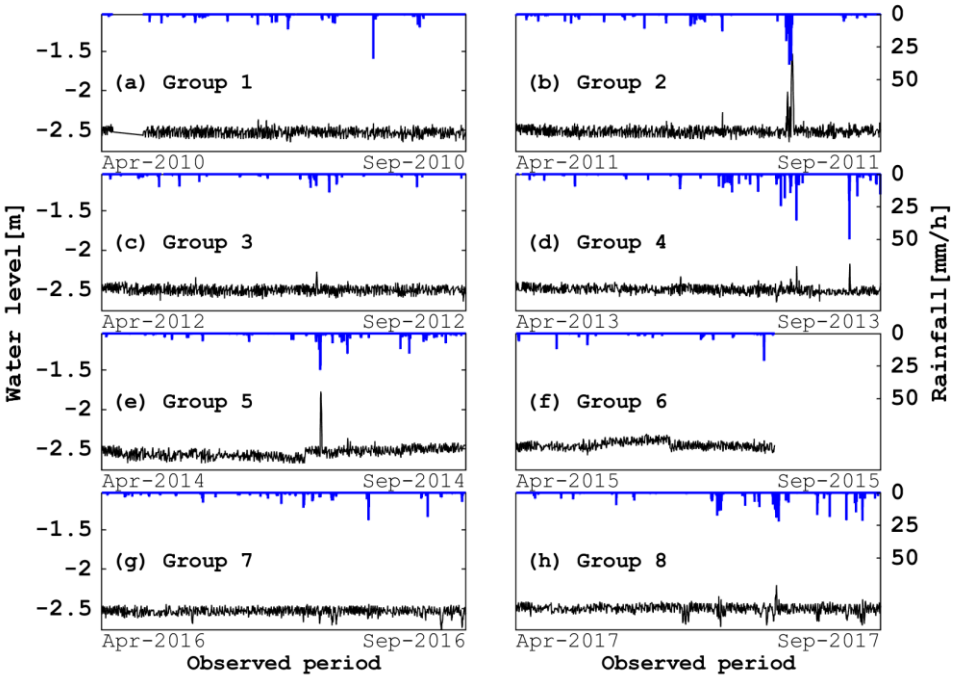

Figure 5. Observed water level and rainfall at D1 during April to August of each group.

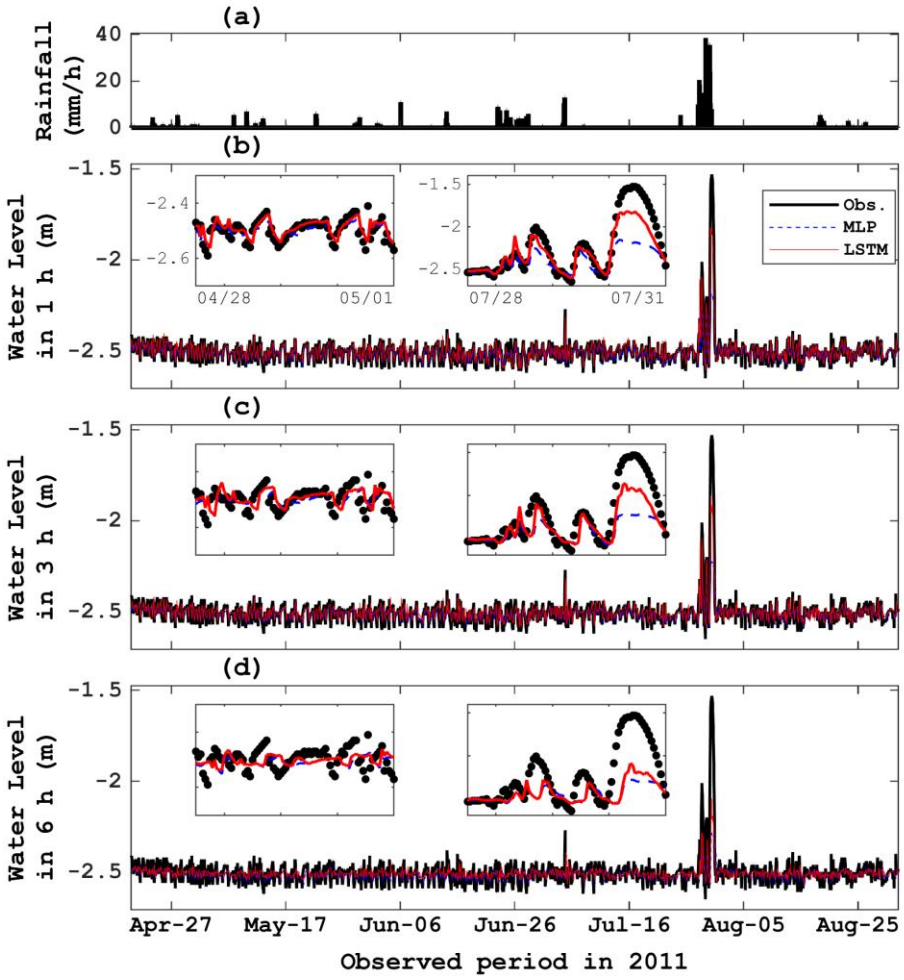

Figure 6. Predicted water levels of Cases 0 and 1 compared with observed data at D1 in G2. (a) rainfall and (b) to (d) indicate water levels in 1 h-, 3 h-, and 6 h- lead times. Two small panels show water levels in the normal pumping and flood-control pumping operations, respectively.

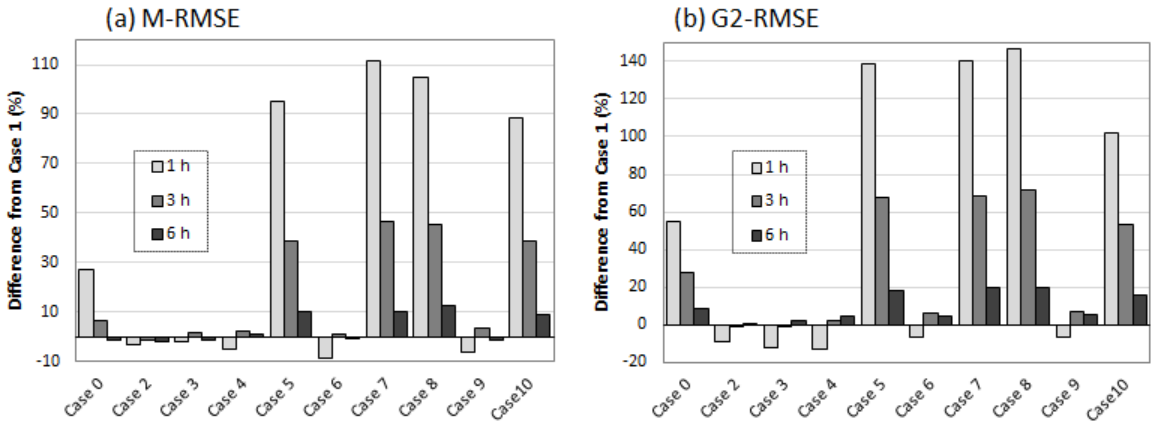

Figure 7. Differences between Case 1 and the other cases in 1 h-, 3 h-, and 6 h-lead times, showing (a) mean RMSEs among all groups and (b) RMSEs in group 2. The negative values indicate the reduction in RMSE when compared with Case 1.

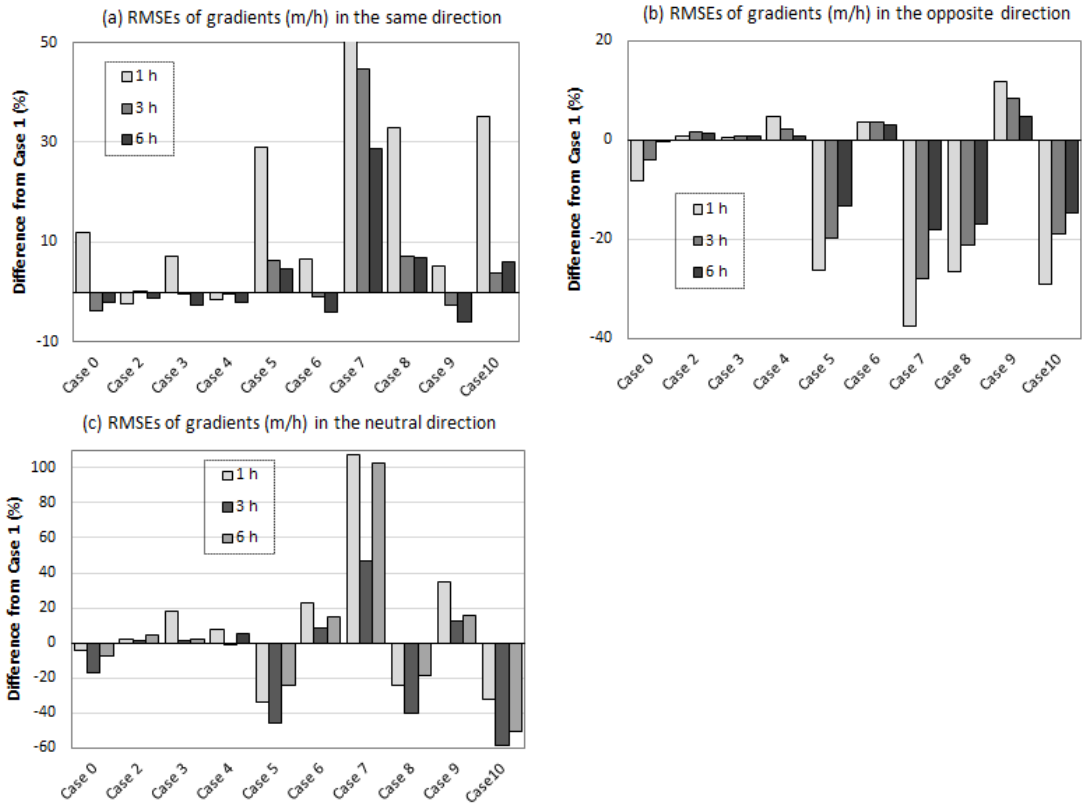

Figure 8. The differences with (a) the same, (b) opposite, and (c) neutral directions across time axis in the M-RMSEs of gradients of water level in the three lead times. Note that 1 h-lead-time difference in Case 7 in (a) reached about 100%.

4. CONCLUSIONS

This study conducted the model sensitivity tests of input data, provided by the irrigation and drainage pumping stations for the irrigation season, using an advanced deep neural network (LSTM) model. The input data were set up by plural combinations of data items (e.g., water level and rainfall) and observed locations. The accuracy of the model prediction of water level at the pond was evaluated by a cross validation method with RMSEs between model and observation and by measures of shape differences of water level with gradient directions. We revealed that a better prediction of water level at the pond was provided by Case 2 with I1–I4 and D1 pumping stations with the data items: water level, rainfall, and discharge. In addition, water level was a key variable as input data to minimize the errors.

ACKNOWLEDGMENTS

This research was supported by grants from the Project of the NARO Bio-oriented Technology Research Advancement Institution. We greatly appreciate the local land improvement district, a local government, MAFF Japan, and MLIT Japan for the observed data acquisition.

REFERENCES

Geisser, S. (1993). Predictive inference: An introduction, Monographs on statistics and applied probability 55. Chapman and Hall, NY, USA, pp. 240.

Hitokoto, M., Sakuraba, M. and Sei, Y. (2016). Development of the real-time river stage prediction method using deep learning. *Journal of Japan Society of Civil Engineers* (*JSCE*), *Series B1* (*hydraulic engineering*), 72(4):I_187–I_192. (In Japanese) doi:10.2208/journalofjsce.5.1_422.

Hochreiter, P. and Schmidhuber, J. (1997). Long short-term memory. *Neural Computation*, 9(8):1735–1780. doi:10.1162/neco.1997.9.8.1735.

Hu, C., Wu, Q., Li, H., Jian, S., Li, N. and Lou, Z. (2018). Deep learning with a long short-term memory networks approach for rainfall-runoff simulation. Water, 10:1543. doi:10.3390/w10111543.

Kimura, N., Nakata, T., Kiri, H., Sekijima, K., Azechi, I., Yoshinaga, I. and Baba D. (2019). Water level prediction at drainage pump station in low lands using LSTM model. *Journal of JSCE Ser. B1* (*hydraulic. engineering*), 75:I_235–I_240. (In Japanese)

Kimura, N., Yoshinaga, I, Sekijima, K., Azechi, I., Kiri, H., and Baba D. Artificial neural network predictions for water levels at drainage pumping stations in an agricultural lowland. Submitted to *Japan Agricultural Research Quarterly*.

Le, X., Ho, H. V., Lee, G. and Jung, S. (2019). Application of long short-term memory (LSTM) neural network for flood forecasting. *Water*, 11:1387. doi:10.3390/w11071387.

McCulloch, W. S. and Pitts, W. (1943). A logical calculus of the ideas immanent in nervous activity. *Bulletin of mathematical biophysics*, 5(4):115–133. doi:10.1007/BF02478259

Yamada, K., Kobayashi, Y., Nakatsugawa, M. and Kishigami, J. (2018). A case study of flood water level prediction in the Tokoro River in 2016 using recurrent neural networks. *Journal of JSCE Ser. B1* (*hydraulic. engineering*), 74(5):I_1369–I_1374. (In Japanese) doi:10.2208/jscejhe.74.5_I_1369